

The filled skutterudite $\text{CeOs}_4\text{As}_{12}$: a hybridization gap semiconductor

R. E. Baumbach^{*}, P. C. Ho[†], T. A. Sayles^{*}, M. B. Maple^{*}, R. Wawryk[‡], T. Cichorek[‡], A. Pietraszko[‡], and Z. Henkie[‡]

^{*}Department of Physics and Institute for Pure and Applied Physical Sciences, University of California at San Diego, La Jolla, CA 92093, USA, [†]Department of Physics, California State University, Fresno, Fresno, CA 93740, USA, and [‡]Institute of Low Temperature and Structure Research, Polish Academy of Sciences, 50-950 Wrocław, Poland

Submitted to Proceedings of the National Academy of Sciences of the United States of America

– X-ray diffraction, electrical resistivity, magnetization, specific heat, and thermoelectric power measurements are presented for single crystals of the new filled skutterudite compound $\text{CeOs}_4\text{As}_{12}$, which reveal phenomena that are associated with f - electron - conduction electron hybridization. Valence fluctuations or Kondo behavior dominates the physics down to $T \sim 135$ K. The correlated electron behavior is manifested at low temperatures as a hybridization gap insulating state. The small energy gap $\Delta_1/k_B \sim 73$ K, taken from fits to electrical resistivity data, correlates with the evolution of a weakly magnetic or nonmagnetic ground state, which is evident in the magnetization data below a coherence temperature $T_{coh} \sim 45$ K. Additionally, the low temperature electronic specific heat coefficient is small, $\gamma \sim 19$ mJ/mol K². Some results for the nonmagnetic analogue compound $\text{LaOs}_4\text{As}_{12}$ are also presented for comparison purposes. –

filled skutterudite | $\text{CeOs}_4\text{As}_{12}$ | hybridization gap insulator

Introduction

The ternary transition metal pnictides with the chemical formula MT_4X_{12} (M = alkali metal, alkaline earth, lanthanide, actinide; T = Fe, Ru, Os; X = P, As, Sb) which crystallize in the filled skutterudite structure (space group $\text{Im}\bar{3}$) exhibit a wide variety of strongly correlated electron phenomena.[1, 2, 3, 4] Many of these phenomena depend on hybridization between the rare earth or actinide f - electron states and the conduction electron states which, in some filled skutterudite systems, leads to the emergence of semiconducting behavior. This trend is evident in the cerium transition metal phosphide and antimonide filled skutterudite systems, most of which are semiconductors where the gap size is correlated with the lattice constant.[5, 6, 7] While these systems have been studied in detail, the arsenide analogues have received considerably less attention, probably due to materials difficulties inherent to their synthesis. In this paper, we present new measurements of electrical resistivity ρ , magnetization M , specific heat C , and thermoelectric power S which show that $\text{CeOs}_4\text{As}_{12}$ has a nonmagnetic or weakly magnetic semiconducting ground state with an energy gap Δ in the range $45 \text{ K} \leq \Delta/k_B \leq 73 \text{ K}$ and a small electronic specific heat coefficient $\gamma \sim 19$ mJ/mol K². Thus, we suggest that $\text{CeOs}_4\text{As}_{12}$ may be a member of the class of compounds, commonly referred to as hybridization gap semiconductors or, in more modern terms, Kondo insulators. In these materials the localized f - electron states hybridize with the conduction electron states to produce a small gap ($\sim 1 - 10$ meV) in the electronic density of states. Depending on the electron concentration, the Fermi level can be found within the gap, yielding semiconducting behavior, or outside the gap, giving metallic heavy fermion behavior. For a more complete discussion of the topic, we refer the reader to several excellent reviews.[8, 9] For comparison purposes, we also report results for the weakly magnetic analogue material $\text{LaOs}_4\text{As}_{12}$.

Experimental Details

Single crystals of $\text{CeOs}_4\text{As}_{12}$ and $\text{LaOs}_4\text{As}_{12}$ were grown from elements with purities $\geq 99.9\%$ by a molten metal flux method at high temperatures and pressures, as reported elsewhere.[10] After removing the majority of the flux by distillation, $\text{CeOs}_4\text{As}_{12}$ single crystals with dimensions up to ~ 0.7 mm and $\text{LaOs}_4\text{As}_{12}$ single crystals with dimensions up to ~ 0.3 mm were collected and cleaned in acid in an effort to remove any impurity phases from the surfaces of the crystals. The crystal structure of $\text{CeOs}_4\text{As}_{12}$ was determined by X-ray diffraction on a crystal with dimensions of $0.28 \times 0.25 \times 0.23$ mm. A total of 5757 reflections (454 unique, $R_{int}=0.1205$) were recorded and the structure was resolved by the full matrix least squares method using the SHELX-97 program.[11, 12] A similar measurement was made for the $\text{LaOs}_4\text{As}_{12}$ crystals.

Electrical resistivity $\rho(T)$ measurements for temperatures $T = 65$ mK - 300 K and magnetic fields $H = 0 - 9$ T were performed on the $\text{CeOs}_4\text{As}_{12}$ crystals in a four-wire configuration using a conventional ⁴He cryostat and a ³He - ⁴He dilution refrigerator. Magnetization $M(T)$ measurements for $T = 1.9$ K - 300 K and $H = 0 - 5.5$ T were conducted using a Quantum Design Magnetic Properties Measurement System on mosaics of both $\text{CeOs}_4\text{As}_{12}$ ($m = 154.2$ mg) and $\text{LaOs}_4\text{As}_{12}$ ($m = 138.9$ mg) crystals, which were mounted on a small Delrin disc using Duco cement. Specific heat $C(T)$ measurements for $T = 650$ mK - 18 K and $H = 0$ and 5 T were made using a standard heat pulse technique on a collection of 116 single crystals ($m = 65$ mg) of $\text{CeOs}_4\text{As}_{12}$ which were attached to a sapphire platform with a small amount of Apiezon N grease in a ³He semiadiabatic calorimeter. Thermoelectric power $S(T)$ measurements for $T = 0.5$ K - 350 K for $\text{CeOs}_4\text{As}_{12}$ single crystals was determined by a method described elsewhere.[13]

Results

Single crystal structural refinement shows that the unit cells of $\text{CeOs}_4\text{As}_{12}$ and $\text{LaOs}_4\text{As}_{12}$ have the $\text{LaFe}_4\text{P}_{12}$ - type structure ($\text{Im}\bar{3}$ space group) with two formula units per unit cell, and room temperature lattice constants $a = 8.519(2)$ Å and $a = 8.542(1)$ Å, respectively, in reasonable agreement with earlier measurements of $a = 8.5249(3)$ Å and $a = 8.5296$ Å for $\text{CeOs}_4\text{As}_{12}$ and $a = 8.5437(2)$ Å for $\text{LaOs}_4\text{As}_{12}$. [6, 14] Other

Reserved for Publication Footnotes

crystal structure parameters for these compounds are summarized in Table I. The displacement parameter D represents the average displacement of an atom vibrating around its lattice position and is equal to its mean-square displacement along the Cartesian axes. The displacement parameters determined for CeOs₄As₁₂ and LaOs₄As₁₂ are typical of the lanthanide filled skutterudites.[15, 16] Table I also indicates that the Ce sites in CeOs₄As₁₂ may not be fully occupied, as is often the case for filled skutterudite materials. By comparison to other lanthanide filled skutterudite arsenides, the lattice constant of CeOs₄As₁₂ is reduced from the expected lanthanide contraction value, indicating that the Ce³⁺ 4f electron states are strongly hybridized with the conduction electron states of the surrounding Os and As ions.

Electrical resistivity data for a typical CeOs₄As₁₂ single crystal specimen for $T = 65$ mK - 300 K and $H = 0$ and a polycrystalline LaOs₄As₁₂ reference specimen[17] are shown in Fig. 1. For $H = 0$ T, $\rho(T)$ for CeOs₄As₁₂ decreases weakly with T from a value near 1 mΩcm at 300 K to 0.5 mΩcm at 135 K, below which $\rho(T)$ increases continuously to low T . An extremely broad hump centered around ~ 15 K is superimposed on the increasing $\rho(T)$ which saturates below 300 mK towards a constant value near 100 mΩcm. Above 135 K, $\rho(T)$ for CeOs₄As₁₂ is similar to that of polycrystalline LaOs₄As₁₂. However, below 135 K, LaOs₄As₁₂ continues to exhibit metallic behavior, wherein $\rho(T)$ saturates near 0.1 mΩcm before undergoing an abrupt drop at the superconducting transition near 3.2 K. With the application of a magnetic field (left Fig. 1 inset), $\rho(T)$ for CeOs₄As₁₂ increases for $3 \text{ K} \leq T \leq 300 \text{ K}$ by a small and nearly temperature independent amount and the broad hump moves towards lower T . Below ~ 3 K, $\rho(T)$ for CeOs₄As₁₂ is drastically affected by H , where the residual resistivity, ρ_0 , is reduced by more than a factor of 10 with $H = 5$ T. For fields greater than 5 T, the relative effect of increasing magnetic field on $\rho(T)$ is less pronounced, as ρ_0 saturates near 6 mΩcm. Finally, it should be noted that the residual resistivity for $H = 9$ T is slightly larger than that for $H = 7$ T.

DC magnetization data, $\chi(T) = M(T)/H$, collected in a small constant field $H = 0.5$ kOe, are shown in Fig. 2 for CeOs₄As₁₂ and LaOs₄As₁₂. For CeOs₄As₁₂, $\chi(T)$ shows a weak and unusual T dependence. Below 300 K, $\chi(T)$ decreases with decreasing T , suggesting a maximum above 300 K. Below a first minimum at $T \sim 135$ K, $\chi(T)$ increases with decreasing T down to $T_{\chi,0} \sim 45$ K, where it again decreases with decreasing T down to ~ 20 K. Near 20 K, $\chi(T)$ show a second minimum, below which a weak upturn persists down to 1.9 K with a small feature between 2 and 4 K. The minimum in $\chi(T)$ near 135 K roughly corresponds to the temperature where $\rho(T)$ begins to increase with decreasing T . The low T upturn in $\chi(T)$ is weakly suppressed in field, as reflected in the low temperature M vs H isotherms (not shown) which have weak negative curvature, and only begin to show a tendency towards saturation above ~ 30 kOe. No hysteretic behavior is observed. Similar measurements for LaOs₄As₁₂ at $T = 1.9$ K reveal that the low T magnetic isotherm is linear in field up to 55 kOe. The magnetic susceptibility of LaOs₄As₁₂ is of comparable magnitude to that of CeOs₄As₁₂, and shows a weak increase with decreasing T down to the superconducting transition temperature $T_c \sim 3.2$ K, as is typical for many La based compounds for which $\chi(T)$ often has a weak temperature dependence.[18]

Displayed in Fig. 3 are specific heat divided by temperature $C(T)/T$ vs T^2 data for $T = 650$ mK - 18 K in magnetic fields $H = 0$ and 5 T. For 650 mK $< T < 7$ K, $C(T)/T$ is described by the expression,

$$C(T)/T = \gamma + \beta T^2 \quad [1]$$

where γ is the electronic specific heat coefficient and $\beta \propto \theta_D^{-3}$ describes the lattice contribution. Fits of eq. 1 to the zero field $C(T)/T$ data show that $\gamma(H = 0) \sim 19$ mJ/mol K² and $\theta_D(H = 0) \sim 264$ K. In contrast to $\rho(T)$, the application of a 5 T magnetic field has only a modest affect on $C(T)/T$, for which γ remains constant while θ_D increases to ~ 287 K. It should also be noted that a small deviation from the linear behavior is seen at $T^2 \sim 40$ K² ($T \sim 6$ K), as shown in the Fig. 3 inset.

The thermoelectric power $S(T)$ data for CeOs₄As₁₂ and LaOs₄As₁₂ are shown in Fig. 4. Near 300 K, $S(T)$ for CeOs₄As₁₂ is positive and one order of magnitude larger than that for metallic LaOs₄As₁₂, which is shown here for reference and studied in greater detail elsewhere.[18] From room T , the thermoelectric power for CeOs₄As₁₂ increases with decreasing T to a maximum value $S_{MAX} = 83$ μV/K at $T_{MAX} = 135$ K, close to the T where semiconducting behavior is first observed in the $\rho(T)$ data. The $S(T)$ data then decrease with decreasing T down to a minimum $S_{min} = 31$ μV/K at $T_{min} = 12$ K, close to the maximum of the broad hump in $\rho(T)$. Additionally, there is a broad peak superimposed on the decreasing $S(T)$ for $T = 12$ K - 60 K. Below 12 K, the $S(T)$ data go through a second maximum $S_{max} = 46$ μV/K at $T_{max} = 2$ K and finally continue to decrease down to 0.5 K, but remain positive.

Discussion

When viewed globally, measurements of x-ray diffraction, $\rho(T)$, $M(T)$, $C(T)/T$, and $S(T)$ indicate that strong f - electron - conduction electron hybridization dominates the physics of CeOs₄As₁₂, yielding a variety of types of behavior which can be roughly divided into high ($T \geq 135$ K) and low ($T \leq 135$ K) temperature regions. For $T > 135$ K, the unusual behavior is most pronounced in the $\chi(T)$ data, which deviate from the typical Curie - Weiss T - dependence expected for Ce³⁺ ions and instead decrease with decreasing T to a broad minimum near $135 \text{ K} \leq T \leq 150$ K. Although it is difficult to definitively determine the origin of this T - dependence, possible mechanisms include valence fluctuations and Kondo behavior. In the valence fluctuation picture, which was introduced to account for the nonmagnetic behavior of α - Ce,[19] SmS in its collapsed “gold” phase,[20] and SmB₆,[21] the 4f electron shell of each Ce ion temporally fluctuates between the configurations 4f¹ (Ce³⁺) and 4f⁰ (Ce⁴⁺) at a frequency $\omega \approx k_B T_{vf}/\hbar$, where T_{vf} separates magnetic behavior at high temperatures $T \gg T_{vf}$ and nonmagnetic behavior at low temperatures $T \ll T_{vf}$. In this phenomenological model, the decrease in $\chi(T)$ with decreasing T can be accounted for in terms of an increase in the Ce ion valence $v(T)$ with decreasing T towards 4+, corresponding to a decrease in the average 4f electron shell occupation number $n_{4f}(T)$ towards zero. At $T = 0$ K, $\chi(T)$ should be approximately,

$$\chi(0) \approx \frac{n_{4f^0}(T)\mu_{eff}^2(4f^0) + n_{4f^1}(T)\mu_{eff}^2(4f^1)}{3k_B(T + T_{vf})}|_{T=0} \quad [2a]$$

$$= \frac{n_{4f^1}(0)\mu_{eff}^2(4f^1)}{3k_B(T_{vf})} \quad [2b]$$

since $\mu_{eff}(4f^0) = 0$. In this model, the value of T_{sf} can be estimated from the Curie - Weiss behavior of $\chi(T)$ for $T \gg T_{sf}$ where it plays the role of the Curie - Weiss temperature, and $n_{4f^1}(0)$ can be inferred from $\chi(0)$. Since the Curie - Weiss behavior would be well above room T for this case, it is not possible to estimate T_{sf} and $n_{4f^1}(T)$. The behavior of $n_{4f^1}(0)$

can also be deduced from measurements of the lattice constant a as a function of T , by x - ray diffraction or thermal expansion measurements. The increase in valence with decreasing T is reminiscent of the γ - α transition in elemental Ce, in which the valence undergoes a transition towards 4+ with decreasing T that is discontinuous (1st order) for pressures $P < P_c$ where P_c is the critical point, and continuous (2nd order) for $P > P_c$. According to this picture, it would appear that the critical point for CeOs₄As₁₂ is at a negative pressure and the valence is increasing with decreasing T . A great deal of effort has been expended to develop a microscopic picture of the intermediate valence state, and the reader is referred to two of many review articles on the subject.[22, 23]

In contrast to the intermediate valence picture, it is possible that the Ce ions remain in the 3+ state at all T , and the Ce³⁺ magnetic moments are screened by the conduction electron spins below a characteristic temperature T_K . This scenario is commonly called the Kondo picture,[24] and may be appropriate for CeOs₄As₁₂ if $T_K > 300$ K, leading to Curie - Weiss behavior for $T > T_K$ and the observed $\chi(T)$ behavior for $135 \text{ K} < T < T_K$. A rough approximation of T_K can be made using the expression,

$$T_K = N_A \mu_{eff}^2 / 3 \chi_0 k_B \quad [3]$$

where $\mu_{eff} = 2.54 \mu_B$ is the Hund's rule value for Ce³⁺ ions and $\chi_0 \sim 1.2 \times 10^{-3} \text{ cm}^3/\text{mol}$ is the saturated value of $\chi(T)$ at $T \sim 135$ K, representing the magnetic susceptibility of a screened Kondo ion singlet.[25] Using this rough expression, T_K is found to be near 670 K, supporting the notion of a high Kondo temperature. Moreover, if the Kondo interpretation with a high T_K is correct, the decrease of $\rho(T)$ with decreasing T may reflect the onset of Kondo coherence above 300 K, in addition to the freezing out of phonons. Finally, it is worth noting that the $\chi(T)$ data for LaOs₄As₁₂ indicate that spin fluctuations associated with the transition metal atoms do not account for the unusual $\chi(T)$ behavior seen for CeOs₄As₁₂.

The affects of f - electron - conduction electron hybridization become even more pronounced below 135 K, where $\rho(T)$ evolves into a gapped semiconducting state which persists to the lowest T measured. The increase in $\rho(T)$ is not well described by a simple Arrhenius function, as would be expected for a semiconductor with a single energy gap. Instead, the following phenomenological expression,[26]

$$\rho^{-1}(T) = \sum_{i=0}^3 A_i \exp(-\Delta_i/k_B T) \quad [4]$$

where $A_1 = 2.7 (\text{m}\Omega\text{cm})^{-1}$, $\Delta_1/k_B = 73$ K, $A_2 = 0.44 (\text{m}\Omega\text{cm})^{-1}$, $\Delta_2/k_B = 16$ K, $A_3 = 0.18 (\text{m}\Omega\text{cm})^{-1}$ and $\Delta_3/k_B = 2.51$ K, describes the data for $1 \text{ K} \leq T \leq 135$ K, as shown in the right Fig. 1 inset. A possible interpretation of this fit is that the large gap Δ_1 describes the intrinsic energy gap for CeOs₄As₁₂ while Δ_2 and Δ_3 describe impurity donor or acceptor states in the gap (Kondo holes),[27, 28, 29] or, possibly, a pseudogap. In this situation, it is naively expected that the application of a magnetic field will act to close the energy gaps (Δ_1 , Δ_2 , Δ_3) through the Zeeman interaction,

$$\Delta_n(H) = \Delta_n(H=0) - g_J |J_z| \mu_B H \quad [5]$$

where $\Delta_n(H=0)$ are the zero field gaps, $g_J = 6/7$ is the Landé g factor for Ce³⁺ ions, $J_z = 5/2$ is the z component of the total angular momentum for Ce³⁺ ions, and μ_B is the Bohr magneton. According to this expression, it is expected that a field $H = \Delta_n(H=0)/g_J |J_z| \mu_B \sim 1.74$ T is sufficient

to close the low T gap. This behavior is qualitatively shown in the left Fig. 1 inset where the low T resistivity is reduced by nearly 70 % for $H = 1.5$ T.

Concurrent with the emergence of the semiconducting behavior, $\chi(T)$ increases slowly down to $T_{\chi,0} \sim 45$ K, where it goes through a maximum and then continues to decrease with decreasing T . Therefore, there is an apparent correlation between the intrinsic energy gap value $\Delta_1 \sim 73$ K taken from fits to $\rho(T)$ and the broad maximum in $\chi(T)$ centered around $T_{\chi,0} \sim 45$ K. If $T_{\chi,0}$ is taken to indicate the onset of a coherent non-magnetic ground state where $T_{\chi,0} \sim T_{coh} \sim \Delta_1/k_B$, then the likely description of the ground state is the well known many body hybridization gap picture, where the magnetic moments of the Ce³⁺ f - electron lattice are screened by conduction electron spins via an antiferromagnetic exchange interaction.

In the context of this model, the weak upturn in $\chi(T)$ for $T < 20$ K is unexpected. For this reason, it is necessary to consider whether it is intrinsic or extrinsic to CeOs₄As₁₂. As shown in the inset to Fig. 2, various functions describe the T - dependence of the upturn below ~ 10 K, including both power law and logarithmic functions of the forms,

$$\chi(T) = aT^{-m} \quad [6]$$

and

$$\chi(T) = b - c \ln(T) \quad [7]$$

where $a = 1.96 \times 10^{-3} \text{ cm}^3 \text{ K}^m/\text{mol}$ and $m = 0.16$, or $b = 1.92 \times 10^{-3} \text{ cm}^3/\text{mol}$ and $c = 0.25 \times 10^{-3} \text{ cm}^3/\text{mol}$, respectively. These weak power law and logarithmic divergences in T of physical properties are often associated with materials that exhibit non-Fermi liquid behavior due to the proximity of a quantum critical point.[30, 31, 32] On the other hand, it is also possible that the upturn is the result of paramagnetic impurities, as is often found for hybridization gap semiconductors.[9, 33] To address this possibility, the low T upturn in $\chi(T)$ was fitted using a Curie - Weiss function of the form,

$$\chi(T) = \chi_0 + C_{imp}/(T - \Theta) \quad [8]$$

where $\chi_0 = 1.13 \times 10^{-3} \text{ cm}^3/\text{mol}$, $C_{imp}(T) = 3.12 \times 10^{-3} \text{ cm}^3 \text{ K}/\text{mol}$, and $\Theta = -3$ K. Although it is not possible, by means of this measurement, to quantitatively determine the origin of such an impurity contribution, a rough estimate of the impurity concentration can be made by assuming that it is due to paramagnetic impurity ions, such as rare earth ions like Ce³⁺ or Gd³⁺, which give impurity concentrations near 0.4 % and 0.04% respectively. Finally, to elucidate the significance of an impurity contribution of this type, the hypothetical intrinsic susceptibility $\chi_{int}(T) = \chi(T) - \chi_{imp}(T)$ is shown in Fig. 2. The resulting $\chi_{int}(T)$ remains nearly identical to $\chi(T)$ down to ~ 100 K, where the affect of $\chi_{imp}(T)$ becomes apparent. Near 55 K, $\chi_{int}(T)$ goes through a weak maximum and then saturates towards a value near $1.1 \times 10^{-3} \text{ cm}^3/\text{mol}$ with decreasing T , consistent with the onset of Kondo coherence leading to a weakly magnetic or nonmagnetic ground state.

Additionally, the behavior of $C(T)/T$ at low T supports the hybridization gap interpretation, for which the low T electronic specific heat coefficient $\gamma = C/T$ is expected to be zero in the fully gapped scenario, or small and finite if a low concentration of donor or acceptor levels are present or if there is a pseudogap.[34] Similar results were seen for the archetypal hybridization gap semiconductor Ce₃Bi₄Pt₃, for which $\gamma \sim 3.3 \text{ mJ}/(\text{mol Ce K}^2)$. For hybridization gap semiconductors, this value is expected to be sample dependent and to correlate with the number of impurities in the system.[9, 35] Similar sample dependence has been observed in both $\rho(T)$ and

$C(T)/T$ measurements for $\text{CeOs}_4\text{As}_{12}$ specimens. Moreover, a comparison to other systems where large effective masses are seen as the result of many body enhancements can be made by computing an effective Wilson-Sommerfeld ratio $R_W = (\pi^2 k_B^2 / 3\mu_{eff}^2)(\chi/\gamma)$. The values χ , χ_{int} , and γ are taken at 1.9 K to probe the low temperature state. Also, the Hund's rule effective magnetic moment $\mu_{eff} = 2.54 \mu_B$ for Ce^{3+} ions is used. From these values, R_W is calculated to be ~ 1.04 and ~ 0.67 , for the χ and χ_{int} cases. As expected, these values are similar to those found in f-electron materials where the low T transport and thermodynamic properties are due to conduction electrons with or without enhanced masses.

The T dependence of the thermoelectric power provides further insight into the hybridization gap picture. Since $S(T)$ remains positive over the entire T range, it appears that charge carriers excited from the top of the valence band to the conduction band dominate the transport behavior for all T . However, a single energy gap and charge carrier picture does not adequately describe the T dependence of the data. Instead, there are several unusual features which include, (1) $T_{MAX} = 135$ K, which corresponds to the high T transition in $\rho(T)$ from semimetallic to metallic behavior, (2) $T_{min} = 12$ K, which is close to the low T portion of the extremely broad hump superimposed on $\rho(T)$, and (3) $T_{max} = 2$ K, which is close to Δ_3/k_B . Thus, there is a close correspondence between the deviations from a single energy gap picture between $S(T)$ and $\rho(T)$, although the deviations are more pronounced in $S(T)$ since electrons and holes make contributions of opposite sign to the total $S(T)$. To further characterize $S(T)$, it is useful to consider the expression,[36]

$$S(T) = -P(\mu_n, \mu_p)(k_B/e)(\Delta/2k_B T) + Q \quad [9]$$

which describes intrinsic effects in $S(T)$ for a gapped system, such as activation of electrons from the lower band to the higher one, which creates both hole and electron charge carriers. For this expression, the coefficients $P(\mu_n, \mu_p) = (\mu_n - \mu_p)/(\mu_n + \mu_p)$ and $Q = - (k_B/e)[(a/2k_B) - 2] - (3/4)\ln(m_n/m_p)$, are defined by the electron mobility μ_n , hole mobility μ_p , the temperature coefficient a of Δ vs T , the electron effective mass m_n , and the hole effective mass m_p . Since the quantity $Q(a, m_n, m_p)$ is expected to be weakly T dependent, this expression is a useful tool for identifying energy gap behavior, as was the case for the semiconductor Th_3As_4 . [37] However, as shown in the left Fig. 4 inset, there is only one T range, $6.5 \text{ K} \leq T \leq 15 \text{ K}$, where this type of behavior is observed. A linear fit to $S(T)$ in this T range yields $\Delta/k_B = 2.2 \text{ K}$, which is of the order of Δ_3/k_B found by fits to $\rho(T)$. To further characterize $S(T)$, it is also of interest to consider dS/dT vs $\log T$ (not shown), which was used previously to an-

alyze the compound $\text{Ce}_x\text{Y}_{1-x}\text{Cu}_{2.05}\text{Si}_2$, [38] where a change in the slope was interpreted as evidence for a change of dominant electronic transport mechanism. For $\text{CeOs}_4\text{As}_{12}$, inspection of dS/dT vs $\log T$ yields a characteristic temperature $T^* = 32 \text{ K}$.

Behnia et al. [39] have argued that, in the zero temperature limit, the thermoelectric power should obey the relation,

$$q = (S/T)(N_A e/\gamma) \quad [10]$$

where N_A is Avogadro's number, e is the electron charge and the constant $N_A e = 9.65 \times 10^4 \text{ C mol}^{-1}$ is the Faraday number. The dimensionless quantity q corresponds to the density of carriers per formula unit for the case of a free electron gas with an energy independent relaxation time. Taking the values $S/T = 17.5 \text{ V/K}^2$ and $\gamma = 19 \text{ mJ/mol K}^2$ at $T = 0.5 \text{ K}$ and 0.65 K , respectively, the quantity $q = 89$ is calculated. This value is nearly two orders of magnitude larger than that seen for most of the correlated electron metals analyzed by Behnia et al., but is similar to that found for the Kondo insulator CeNiSn ($q = 107$), for which the Hall carrier density was found to be $0.01/\text{f.u.}$ at 5 K . [39] Thus, the q determined for $\text{CeOs}_4\text{As}_{12}$ is consistent with a related hybridization gap insulator and may be indicative of a low charge carrier density in $\text{CeOs}_4\text{As}_{12}$ at low T .

Summary

The compound $\text{CeOs}_4\text{As}_{12}$ is considered in the context of a simple picture where valence fluctuations or Kondo behavior dominates the physics down to $T \sim 135 \text{ K}$. The correlated electron behavior is manifested at low temperatures as a hybridization gap insulating state, or using modern terminology, as a Kondo insulating state. The size of the energy gap $\Delta_1/k_B \sim 73 \text{ K}$, is deduced from fits to electrical resistivity data and the evolution of a weakly magnetic or nonmagnetic ground state, which is evident in the magnetization data below a coherence temperature $T_{coh} \sim 45 \text{ K}$. Additionally, the low temperature electronic specific heat coefficient is small, $\gamma \sim 19 \text{ mJ/mol K}^2$, as is expected for hybridization gap insulators. The thermoelectric power and electrical resistivity data also indicate that either impurity states in the energy gap or the presence of a pseudogap strongly perturbs the physical behavior away from that of an ideal hybridization gap insulator.

ACKNOWLEDGMENTS. Research at the University of California, San Diego was supported by the U. S. Department of Energy under grant no. DE FG02-04ER46105 and the National Science Foundation under grant no. NSF DMR0335173. Research at ILTSR, Wrocław was supported by the Polish Ministry of Science and Higher Education (Grant No. NN 202 4129 33).

1. M. B. Maple, E. D. Bauer, N. A. Frederick, P.-C. Ho, W. M. Yuhasz, and V. S. Zapf (2003) Strongly correlated electron phenomena in the filled skutterudite compounds. *Physica B* 328: 29.
2. Y. Aoki, H. Sugawara, H. Harima, and H. Sato (2005) Novel Kondo behaviors realized in the filled skutterudite structure. *J. Phys. Soc. Jpn.* 74: 209.
3. M. B. Maple, Z. Henkie, R. E. Baumbach, T. A. Sales, N. P. Butch, P.-C. Ho, T. Yanagisawa, W. M. Yuhasz, R. Wawryk, T. Cichorek, and A. Pietraszko (2008) Correlated electron phenomena in Ce- and Pr- based filled skutterudite arsenides and antimonides. *J. Phys. Soc. Jpn.* 77: 7.
4. H. Sato, D. Kikuchi, K. Tanaka, M. Ueda, H. Aoki, T. Ikeno, S. Tatsuoka, K. Kuwahara, Y. Aoki, M. Koghi, H. Sugawara, K. Iwasa, and H. Harima (2008) Novel features realized in the filled skutterudite structure. *J. Phys. Soc. Jpn.* 77: 1.
5. H. Sugawara, S. Osaki, M. Kobayashi, T. Namiki, S. R. Saha, Y. Aoki, and H. Sato (2005) Transport properties in $\text{CeOs}_4\text{Sb}_{12}$: a possibility of the ground state being semiconducting. *Phys. Rev. B* 71: 125127.
6. D. J. Braun and W. Jeitschko (1980) Ternary arsenides with $\text{LaFe}_4\text{P}_{12}$ structure. *J. Solid State Chem.* 32: 357.
7. D. J. Braun and W. Jeitschko (1980) Preparation and structural investigations of antimonides with the $\text{LaFe}_4\text{P}_{12}$ structure. *J. Less Comm. Met.* 72: 147.
8. Z. Fisk, P. C. Canfield, J. D. Thompson, and M. F. Hundley (1992) $\text{Ce}_3\text{Bi}_4\text{Pt}_3$ and hybridization gap physics. *J. Alloys and Comp.* 181: 369.
9. P. S. Riseborough (2000) Heavy fermion semiconductors. *Adv. Phys.* 49: 257.
10. Z. Henkie, M. B. Maple, A. Pietraszko, R. Wawryk, T. Cichorek, R. E. Baumbach, W. M. Yuhasz, and P.-C. Ho (2008) Crystal growth and properties of the filled skutterudite arsenides. *J. Phys. Soc. Jpn.* 77: 128.
11. G. M. Sheldrick (1985) In Program for the Solution of Crystal Structures. University of Göttingen, Germany.
12. G. M. Sheldrick (1987) in Program for Crystal Structure Refinement. University of Göttingen, Germany.
13. R. Wawryk and Z. Henkie (2001) Low temperature resistivity and thermoelectric power controlled by defects in the USB antiferromagnet. *Phil. Mag. B* 81: 223.
14. C. Sekine, R. Abe, K. Takeda, K. Matsuhiro, and M. Wakeshima (2007) High pressure synthesis of the filled skutterudite arsenide $\text{CeOs}_4\text{As}_{12}$. *Physica B* 403: 856.

15. B. C. Sales, D. Mandrus, B. C. Chakoumakos, V. Keppens, and J. R. Thompson (1997) Filled skutterudite antimonides: electron crystals and phonon glasses. *Phys. Rev. B* 56: 15081.
16. B. C. Sales, B. C. Chakoumakos, D. Mandrus, J. W. Sharp, N. R. Dilley, and M. B. Maple (1999) Atomic displacement parameters: A useful tool in the search for new thermoelectric materials? *Mater. Res. Soc. Symp. Proc.* 545: 13.
17. I. Shirovani, K. Ohno, C. Sekine, T. Yagi, T. Kawakami, T. Nakanishi, H. Takahashi, J. Tang, A. Matsushita, and T. Matsumoto (2000) Electrical conductivity and superconductivity of $\text{LaT}_4\text{As}_{12}$ ($T = \text{Fe, Ru, Os}$) with skutterudite type structure. *Physica B* 281: 1021.
18. R. Wawryk, O. Zogal, A. Pietraszko, S. Paluch, T. Cichorek, W.M. Yuhasz, T. A. Sayles, P.-C. Ho, T. Yanagisawa, N. P. Butch, M. P. Maple, and Z. Henkie (2008) Crystal structure, ^{139}La NMR and transport properties of the As based filled skutterudites $\text{LaOs}_4\text{As}_{12}$ and $\text{PrOs}_4\text{As}_{12}$. *J. Alloys and Comp.* 451: 454.
19. M. R. MacPherson, G. E. Everett, D. Wohlleben, and M. B. Maple (1971) Magnetic susceptibility of Ce metal under pressure. *Phys. Rev. Lett.* 26: 20.
20. M. B. Maple and D. Wohlleben (1974) Demagnetization of rare earth ions in metals due to valence fluctuations. *AIP Conference Proceedings* 18: 447.
21. A. Menth, E. Beuhler, and T. H. Geballe (1969) Magnetic and semiconducting properties of SmB_6 . *Phys. Rev. Lett.* 22:295.
22. M. B. Maple, L. E. DeLong, and B. C. Sales (1978) in *Handbook on the Physics and Chemistry of Rare Earths Volume 1 - Metals*, eds K. A. Gschneider, Jr. and L. R. Wyring (North-Holland Publishing Company, Amsterdam), pp 797-846.
23. A. Jayaraman (1979) in *Handbook on the Physics and Chemistry of Rare Earths Volume 2 - Alloys and Intermetallics*, eds K. A. Gschneider, Jr. and L. R. Wyring (North-Holland Publishing Company, Amsterdam), pp 575-611.
24. A. C. Hewson (1993) *The Kondo Problem to Heavy Fermions* (Cambridge University Press).
25. D. A. Gajewski, N. R. Dilley, E. D. Bauer, E. J. Freeman, R. Chau, M. B. Maple, D. Mandrus, B. C. Sales, and A. Lacerda (1998) Heavy fermion behavior of the cerium filled skutterudites $\text{CeFe}_4\text{Sb}_{12}$ and $\text{Ce}_{0.9}\text{Fe}_3\text{CoSb}_{12}$. *J. Phys.: Cond. Mat.* 10: 6973.
26. N. F. Mott and W. D. Twose (1961) The theory of impurity conduction. *Adv. Phys.* 10: 107.
27. R. Sollie and P. Schlottmann (1991) A simple theory of the Kondo hole. *J. Appl. Phys.* 69: 5478.
28. R. Sollie and P. Schlottmann (1991) Local density of states in the vicinity of a Kondo hole. *J. Appl. Phys.* 70: 5803.
29. P. Schlottmann (1992) Impurity bands in Kondo insulators. *Phys. Rev. B* 46: 998.
30. M. B. Maple, C. L. Seaman, D. A. Gajewski, Y. Dalichouch, V. B. Barbetta, M. C. deAndrade, H. A. Mook, H. G. Lukefahr, O. O. Bernal, and D. E. MacLaughlin, Non Fermi liquid behavior in strongly correlated electron f electron materials. *J. Low Temp. Phys* 95: 225.
31. M. B. Maple, M. C. de Andrade, J. Herrmann, Y. Dalichouch, D. A. Gajewski, C. L. Seaman, R. Chau, R. Movshovich, M. C. Aronson, and R. Osborn (1995) Non Fermi liquid ground states in strongly correlated f electron materials. *J. Low Temp. Phys* 99: 224.
32. G. R. Stewart (2001) Non-Fermi-liquid behavior in d- and f- electron metals. *Rev. Mod. Phys.* 73: 797.
33. M. F. Hundley, P. C. Canfield, J. D. Thompson, and Z. Fisk (1990) Hybridization gap in $\text{Ce}_3\text{Bi}_4\text{Pt}_3$. *Phys. Rev. B* 42: 6842.
34. P. Schlottmann (1993) Impurity states in Kondo insulators. *Physica B* 186-188: 375.
35. M. F. Hundley, P. C. Canfield, J. D. Thompson, and Z. Fisk (1994) Substitutional effects on the electronic transport of the Kondo semiconductor $\text{Ce}_3\text{Bi}_4\text{Pt}_3$. *Phys. Rev. B* 50: 18142.
36. G. Busch and U. Winkler (1956) Bestimmung der Charakteristischen Grssen eines Halbleiters. Edited by *Ergebnisse der Exakten Naturwissenschaften*, Zürich.
37. Z. Henkie and P. J. Markowski (1978) Preparation and semiconducting properties of Th_3As_4 . *J. Phys. Chem. Solids* 39: 39.
38. M. Ocko, C. Gaibel, and F. Steglich (2001) Transport properties of $\text{Ce}_x\text{Y}_{1-x}\text{Cu}_{2.05}\text{Si}_2$: a heavy fermion alloy system on the border of valence fluctuation. *Phys. Rev. B* 64: 195107.
39. K. Behnia, D. Jaccard and J. Flouquet (2004) On the thermoelectricity of correlated electrons in the zero temperature limit. *J. Phys.: Condens. Matter* 16: 5187.

Table 1. Crystal structure data for $\text{LaOs}_4\text{As}_{12}$ and $\text{CeOs}_4\text{As}_{12}$. The atomic coordinates x , y , and $z = 0.25$ for T atoms and 0 for M atoms. The listed quantities are the following; a (\AA) is the unit cell parameter, x , y , and z are the atomic coordinates for the As atoms, O are the occupancy factors for the T, As, and M atoms, $l_{M,T:As}$ (\AA) are the chemical bond lengths M - As and T - As, D ($\text{\AA}^2 \times 10^3$) are the displacement parameters for atoms T, As, M, and $R1/wR2$ are the final discrepancy factors in %.

	$\text{LaOs}_4\text{As}_{12}$	$\text{CeOs}_4\text{As}_{12}$
a	8.542(1)	8.519(2)
x	0.1488	0.1485
y	0.3491	0.3485
z	0	0
O_T	1.00	1.00
O_{As}	1.00	1.00
O_M	1.00	0.99
$l_{M,As}$	3.2416	3.2350
$l_{T,As}$	2.4544	2.4470
D	6; 7; 14	3; 4; 12
$R1/wR2$	3.49/8.55	4.02/11.0

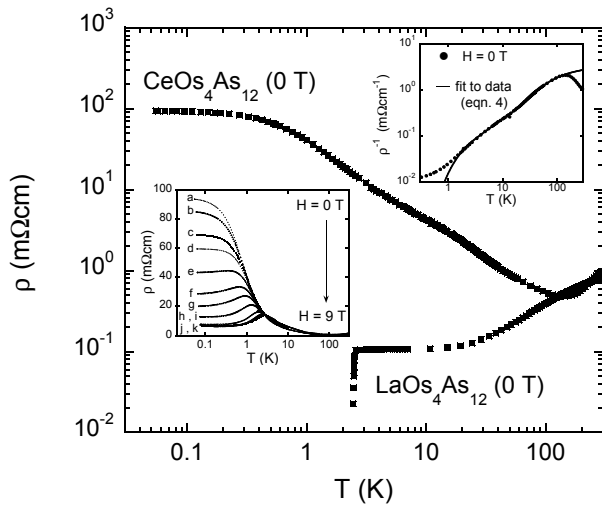


Fig. 1. Electrical resistivity ρ vs temperature T data for $\text{LaOs}_4\text{As}_{12}$ [17] and $\text{CeOs}_4\text{As}_{12}$ for $T = 65 \text{ mK} - 300 \text{ K}$. Right inset close up: The zero field $\rho(T)$ data for $\text{CeOs}_4\text{As}_{12}$ are not described well by an Arrhenius equation which would be appropriate for a simple single gap semiconductor. Instead, the data are described by a three gap expression (eq. 4). Left inset close up: $\rho(T)$ data for $\text{CeOs}_4\text{As}_{12}$ for $T = 65 \text{ mK} - 300 \text{ K}$ and magnetic fields (a) 0 T, (b) 0.3 T, (c) 0.5 T, (d) 0.7 T, (e) 1.0 T, (f) 1.5 T, (g) 2.0 T, (h) 3.0 T, (i) 5.0 T, (j) 7.0 T, and (k) 9.0 T.

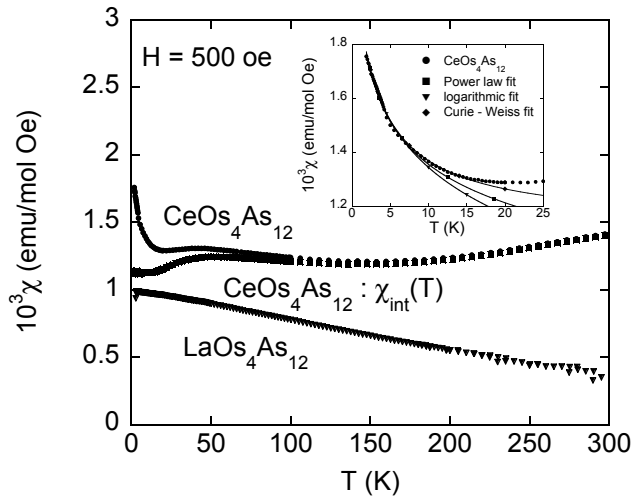


Fig. 2. Magnetic susceptibility $\chi = M/H$ vs temperature T data for $\text{CeOs}_4\text{As}_{12}$ and $\text{LaOs}_4\text{As}_{12}$ for $T = 1.9 \text{ K} - 300 \text{ K}$ and $H = 500 \text{ Oe}$. Also shown is the intrinsic magnetic susceptibility $\chi_{int}(T)$, as defined in the text, for which a Curie - Weiss (CW) impurity contribution has been subtracted. Inset close up: The low T fits to $\chi(T)$ are described by eqs. 6, 7, and 8.

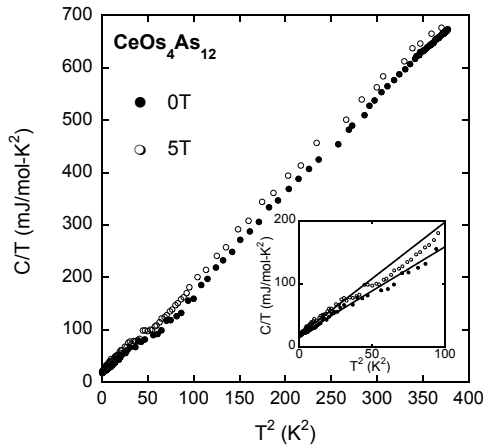


Fig. 3. Specific heat divided by temperature $C(T)/T$ vs temperature squared T^2 data for $\text{CeOs}_4\text{As}_{12}$ for $T = 650 \text{ mK} - 18 \text{ K}$ and in magnetic fields of 0 and 5 T. Inset close up: $C(T)/T$ vs T^2 data for $T = 650 \text{ mK} - 10 \text{ K}$ and in magnetic fields of 0 and 5 T. The straight lines are the fits to the data as described in the text by eqn. 1.

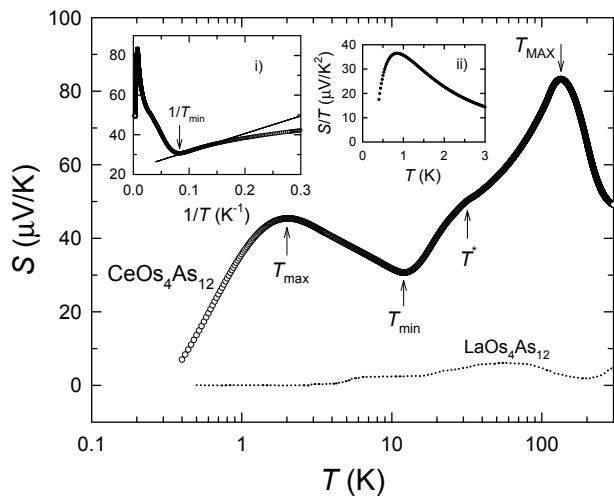


Fig. 4. Thermoelectric power S vs temperature T for $\text{CeOs}_4\text{As}_{12}$ and $\text{LaOs}_4\text{As}_{12}$ for $T = 0.5 \text{ K} - 300 \text{ K}$. Near 300 K , $S(T)$ for $\text{CeOs}_4\text{As}_{12}$ is positive and one order of magnitude larger than that for metallic $\text{LaOs}_4\text{As}_{12}$. Left inset close up: S vs $1/T$ is used in the text to identify an energy gap. Right inset close up: S/T vs T is used to characterize the charge carrier density at low T , as discussed in the text.